JAST, Vol. 5, No. 4, pp 175–182
◯ Iranian Aerospace Society, December 2008

JAST
Journal of Aerospace Science and Technology

Evaluation of 2-D Aeroelastic Models Based on Indicial Aerodynamic Theory and Vortex Lattice Method in Flutter and Gust Response Determination

S.A. Sina [1], M. Kheiri[2], H. Haddadpour[3], H. Razie[4]

Two 2-D aeroelastic models are presented here to determine instability boundary (flutter speed) and gust response of a typical section airfoil with degrees of freedom in pitch and plunge directions. To build these 2-D aeroelastic models, two different aerodynamic theories including Indicial Aerodynamic Theory and Vortex Lattice Method (VLM) have been employed. Also, a 3-D aeroelastic framework constructed using Boundary Element Method (BEM) and modal technique is used to show the accuracy and reliability of the presented 2-D aeroelastic models. The methods reviewed in this study are used to predict the non-dimensional flutter speed and its corresponding frequency for a typical section airfoil (for the 3-D model a high aspect ratio wing with the same cross-sectional characteristics is used) Then, a group of figures show how different time-marching schemes can change the dynamic responses due to the sharp edge gust. Also, a set of figures demonstrate comparisons between the 2-D aeroelastic models, and also, with the 3-D model. As seen from the results presented in this study, 2-D aeroelastic models output a lower non-dimensional flutter speed than the 3-D model. In addition, the dynamic responses due to the sharp edge gust predicted by the 2-D models show larger amplitudes than the 3-D model. This means that since the 2-D aeroelastic models can overestimate the dynamical behavior such as flutter speed and responses to the sharp edge gust, they can be used in the preliminary design steps to reduce the cost and to save time.

INTRODUCTION

In the recent years, significant progress has been made to predict the flutter speed and the forced response of isolated airfoils, cascades of airfoils, wings and even complete aircraft configurations. In the case of simple harmonic motion of an airfoil, as a pioneering work, Theodorsen presented a solution to the unsteady flow which is known as Theodorsen function [1]. This seems to be the first place where the important integrals arising from the wake circulation are identified as Bessel functions. But the main drawback of this work is its limitation to account only for periodic pitching and plunging motions, and therefore, it cannot deal with unsteady phenomena like rapid maneuvers and gust entry. Thus, two different approaches have been developed which were used extensively in solving these types of problems. The first one (from the historical point of view) consists of direct numerical approach to some of the integral equations of the vortex sheet, and the other one employs Fourier-Integral superposition of the linear response of simple harmonic motion. Therefore, Fourier-Integral transform of the Theodorsen function along with curve fitting techniques leads to two important indicial functions called Wagner and

1. *PhD Candidate, Dept. of Aerospace Eng., Sharif Univ. of Tech., Tehran, Iran.*
2. *PhD Candidate, Dept. of Mechanical Eng., McGill University, Canada.*
3. *Associate Professor, Dept. of Aerospace Eng., Sharif Univ. of Tech., Tehran, Iran, Email: Haddadpour@sharif.edu*
4. *MSc. Student, Dept. of Aerospace Eng., Sharif Univ. of Tech., Tehran, Iran.*

Kussner functions. Wagner deals with the response to the step change in the airfoil's angle of attack, and Kussner comes up in the case of response to the sharp edge gust. Then, a solution to the unsteady aerodynamic problem due to an arbitrary motion of the airfoil in the time domain will be obtained through Duhamel superposition integral [2].

Several aerodynamic models have been employed up to now within the numerical methods developed for aeroelasticity problems. These range from classical, incompressible, potential flow to viscous, full Navier-Stokes models. Here we intend to focus on those aerodynamic models which are based on the well-established panel methods. Generally, in these methods, a distribution of singularity elements are obtained according to the governing equations and existing boundary conditions. Thus, from the computational viewpoint, these methods seem to be more economical than those methods which solve the whole flow-field. In this study, two different aerodynamic models based on Vortex Lattice Method (VLM) and Boundary Element Method (BEM) are considered. The first one is a classical method, which relies on developing a distribution of vortices on the surface of the lifting body. An integral representation of any potential flow, which assumes incompressible, inviscid and irrotational flow, in terms of singularity distributions is obtained by applying Green's theorem [3, 4]. The second method is the BEM, in which the boundaries of body immersed in the flow-field will be discretized, and the adapted form of the governing equations will be solved only on its boundaries rather than in the whole flow-field. In fact, BEM will reduce the dimensions of the problem by one. Thus, it will require lower CPU time and cost to handle numerical problems with respect to the other numerical solvers. For more details on this method, its historical development, powerful points and its weaknesses see [5-8].

As a general rule, a numerical aeroelastic method builds a discretized form of governing equations (including structural dynamic and aerodynamic equations) on a computational mesh, and that reduced form marches from one time level to another. For example, Davis and Bendiksen [9] applied a time marching scheme to the two dimensional Euler equations to find the unsteady flow about vibrating airfoils. Moreover, Batina [10] computed the time dependent Euler flow about a complete harmonically deforming aircraft. Almost at the same time, Robinson *et.al.* [11] performed an aeroelastic analysis of wings using the Euler equations with a deforming mesh. Rausch *et.al.* [12] also performed a three dimensional time marching aeroelastic analysis using an unstructured Grid Euler method. Although this approach was relatively straightforward, it was computationally expensive. Furthermore, separate analysis had to be performed for each reduced velocity or mass ratio of interest.

Although a variety of methods and approaches have been presented and developed to reduce computation time and memory usage in the aerodynamic and aeroelastic numerical solutions, these reduction schemes are still very demanding. Hence, a novel method based on the eigenanalysis of unsteady flow has been developed to reduce the numerical computations in aeroelastic problems. In this approach, which is very similar to the modal technique in the structural dynamics, only a small number of modes are used in computations. Therefore, an aeroelastic modal model will be formed with a minimum number of degrees of freedom. This model, which is called Reduced Order Model (ROM), was first presented by Hall [13] in the eigen analysis of the unsteady flow around airfoil, cascade and wing. Then, Romanowski and Dowell [14] used the eigen modes of a time domain Euler code to build Reduced Order Models of flow about isolated airfoils. Moreover, Esfahanian and Behbahaninejad [15] applied ROM to the subsonic unsteady flow about complex configurations using BEM.

In this paper, we use both Indicial Aerodynamic Theory and VLM to simulate unsteady aerodynamics around a 2-D plunging-pitching airfoil. Mainly, we intend to make some comparisons between the exact analytical aerodynamic model and VLM in finding flutter speed and aeroelastic response of the airfoil to the various gust profiles. Also, to verify the accuracy and capability of the present 2-D aeroelastic models in flutter and dynamic response predictions, we compare the results with those coming from the 3-D BEM model coupled with a structural dynamic model based on beam theory. Thus, the remaining parts of the paper are organized as follows:

First, the equations of motion will be addressed; then, each Indicial Aerodynamic Theory, VLM and BEM is presented subsequently. In section 2, a general description for time marching schemes is presented. Then, some numerical results are given to show and verify the accuracy and capability of the present 2-D aeroelastic models in predicting flutter speed and dynamic response.

EQUATIONS OF MOTION

The general form of aeroelastic equations for a typical section is given below:

$$[M]\{\ddot{q}\} + [C]\{\dot{q}\} + [K]\{q\} + q_\infty[Q]\{q\} = 0, \qquad (1)$$

where $[M]$, $[C]$ and $[K]$ are generalized structural mass, damping and stiffness matrices, respectively and $\{q\}$ is the generalized coordinate vector and q_∞ is the dynamic pressure. The generalized structural matrices can be set easily based on the structural modeling

scheme and Lagrange's equation. For example, in the case of a typical section airfoil shown in Figure 1, these matrices are given by [16].

Moreover, the matrix $[Q]$ defines the generalized aerodynamic forces as follows:

$$f_{aero} = q_\infty [Q] \{q\}. \tag{2}$$

Indicial Aerodynamic Theory

The discrete sharp edge gust model used here can be expressed as:

$$w_G(t) = H(t) U_G, \tag{3}$$

where U_G is a measure of gust intensity, and $H(t)$ is the Heaviside's step function. The total lift and pitching moment coefficients can be obtained as [2]:

$$C_l(t) = -2\pi \left[w_G(0)\psi(s) + \int_0^s \frac{dw_G(\sigma)}{dt} \psi(s-\sigma)\, d\sigma \right],$$

$$C_m(t) = b\left(\frac{1}{2} + a\right) C_l(t), \tag{4}$$

where $\psi(s)$ is Kussner function, and s is the reduced time ($s = \frac{Ut}{b}$). A convenient analytical form of the Kussner function, which is represented in a simple exponential form, is attributed to Sears and Sparks [17], and is written as follows:

$$\psi(s) \approx 1 - 0.5e^{-0.13s} - 0.5e^{-1.0s}. \tag{5}$$

Therefore, by substituting Eqs. (4) and (5) in Eq. (1), the governing aeroelastic equations based on the indicial aerodynamic theory will be built.

2-D Vortex Lattice Method

In this method, the airfoil and its wake are divided into panels with the same length. Each panel has one vortex point (ξ_i) and one collocation point (x_i). The vortex point, where the vortex strength is assumed to be concentrated, is located at the quarter of the chord length, and the collocation point is located in three quarter of the chord length. Applying the no-penetration condition yields to the well-known Biot-Savart law as given below [3, 18]:

$$w_i = \sum_{j=1}^{M+N} \frac{\Gamma_j}{2\pi(x_i - \xi_j)}, \qquad i = 1, \ldots, M, \tag{6}$$

where w_i is the downwash at the ith collocation point, and Γ_j is the strength of the jth vortex. Also, M is the number of panels on the airfoil, and N is the number of panels placed on the wake. The downwash vector can be stated in terms of airfoil's plunging (h) and pitching (α) amplitudes as given in Eq. (7):

$$\{w\} = [I_1]_{M\times 2} \begin{Bmatrix} h \\ \alpha \end{Bmatrix} + U [I_2]_{M\times 2} \begin{Bmatrix} h \\ \alpha \end{Bmatrix}, \tag{7}$$

where matrices $[I_1]$ and $[I_2]$ are as follows:

$$[I_1] = \begin{bmatrix} 1 & x_{\frac{3}{4}} - b(1+a) \\ \vdots & \vdots \\ 1 & x_{\frac{3}{4}} - b(1+a) \end{bmatrix}, [I_2] = -\begin{bmatrix} 0 & 1 \\ \vdots & \vdots \\ 0 & 1 \end{bmatrix}. \tag{8}$$

Hence, Eq. (6) can be cast in the matrix form as given in the following equation:

$$\{w\} = \begin{bmatrix} [K_1]_{M\times M} & [K_2]_{M\times N} \end{bmatrix} \begin{Bmatrix} \Gamma_a \\ \Gamma_w \end{Bmatrix}. \tag{9}$$

According to the Kelvin's circulation theorem the time rate of change of circulation around any closed curve consisting of the same fluid elements is zero [18]; therefore, the total circulation has to be constant.

$$\frac{d(\Gamma_a + \Gamma_w)}{dt} = 0. \tag{10}$$

The vortex is shed with the free stream velocity into the wake. So, the latter equation is simplified as below:

$$\frac{\partial \Gamma}{\partial t} + U\frac{\partial \Gamma}{\partial x} = 0. \tag{11}$$

The lift force (L) and the pitching moment ($M_{e.a}$) about the elastic axis are obtained by using the Bernoulli equation as appears below:

$$L = \rho U \sum_{i=1}^{M} \Gamma_i + \rho \sum_{i=1}^{M} \sum_{j=1}^{i} \dot{\Gamma}_j \Delta x_j, \tag{12}$$

$$M_{ea} = \rho U \sum_{i=1}^{M} (\zeta_i - ab)\Gamma_i + \rho \sum_{i=1}^{M} (\zeta_i - ab)\Delta x_i \sum_{j=1}^{i} \dot{\Gamma}_j, \tag{13}$$

where ρ is the flow density, b is the half of the chord length, and ab is the distance of the elastic axis aft of the mid-chord. If one plugs Eqs. (6-13) into the general form of aeroelastic equation (Eq. (1)), it will give the aeroelastic equations based on VLM. Later on the time-marching scheme used to solve these equations is discussed.

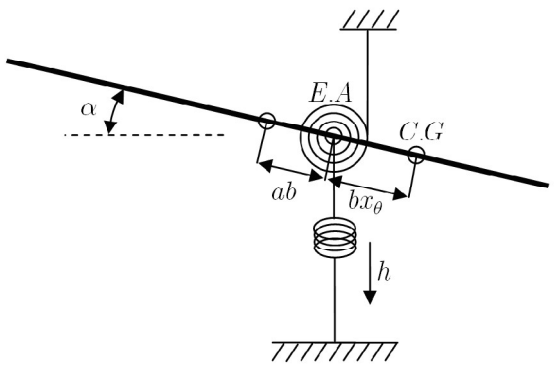

Figure 1. Schematic of a typical airfoil.

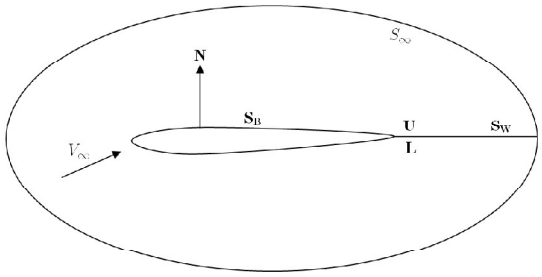

Figure 2. Schematic of the flow-field around a typical body.

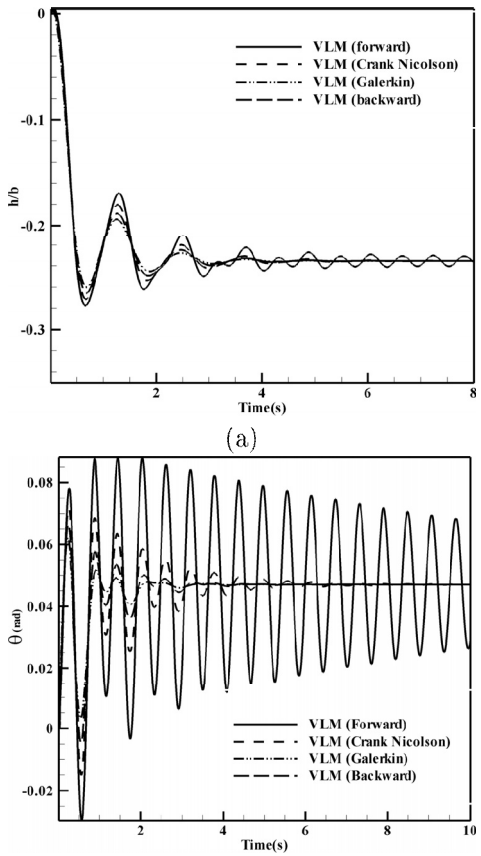

Figure 3. Effect of different time marching schemes on subcritical ($U = 0.75\,U_f$) dynamic responses of the airfoil subjected to a sharp edge gust ($U_g = 0.738\,U_f$): (a) plunging, (b) pitching.

3-D Boundary Element Method

For a flow which is incompressible, ir-rotational and inviscid, the Navier-Stokes equations will reduce to a simple well-known form:

$$\nabla^2\Phi = 0, \tag{14}$$

where Φ is the total velocity potential of the flow-field, and $\nabla^2()$ is the Laplacian operator. Some analytical techniques were developed to solve the potential flow problems, but these can only be applied when major simplifications were made on the geometrical boundary conditions. Hence, some numerical methods have been proposed to solve more realistic geometries whose geometrical boundary conditions will be treated on their actual surface. Panel method is known as a powerful numerical method for flow-field solution around complex configurations. For a general problem like what is shown in Figure 2, the integral form of the governing equation is obtained after some manipulations by applying Green's second identity, and considering the existing boundaries [6]. In addition, it is assumed that each panel located on the body or wake carries a constant velocity potential.

$$2\pi\phi_P = \int_{S_B}\left[\phi\frac{\partial}{\partial\vec{N}}(\frac{1}{r}) - \frac{1}{r}\frac{\partial\phi}{\partial\vec{N}}\right]dS + \int_{S_W}\Delta\phi_W\frac{\partial}{\partial\vec{N}}(\frac{1}{r})dS. \tag{15}$$

Equation 15 gives the velocity potential on an arbitrary panel (ϕ_p) in terms of the influences made by panels located on the body (the first integral on the r.h.s), and those placed on the wake (the second integral on the r.h.s).

This integral form can be cast to a set of algebraic system of equations according to the discretization made on the domain.

$$\phi_{P_h} - \sum_{k=1,k\neq h}^{N_b} c_{hk}\phi_{P_k} - \sum_{k=1}^{N_w} c_{hk}\Delta\phi_{P_k} = \sum_{k=1,k\neq h}^{N_b} d_{hk}(\frac{\partial\phi}{\partial\vec{N}})_{P_k}, \tag{16}$$

The latter formulation gives the perturbed velocity potential on each panel (ϕ_{P_h}) in terms of the potential distributed on all other panels on the body and wake ($\phi_{P_k}, \Delta\phi_{P_k}$), and the downwash ($(\frac{\partial\phi}{\partial\vec{N}})_{P_k}$) induced on the body panels. Also, in this equation, c_{hk} and d_{hk} are influence coefficients, which are computed numerically based on the method presented in [5]. In addition, N_b and N_w are the number of panels placed on the body and wake, respectively, and $\vec{N}$ is the outward unit normal vector of each panel. Some additional equations must be included to find a unique solution. These equations are provided through applying Kutta condition and Kelvin's circulation theorem [6, 8].

TIME MARCHING SCHEMES

Two independent disciplines (aerodynamics and structural dynamics) are brought together through the downwash term and this new coupled set governs the aeroelastic equations [3]. The aeroelastic model according to each aerodynamic model leads to a set of first order time derivative differential equations shown below:

$$[A]\{\dot{\eta}\} + [B]\{\eta\} = \{W\} \tag{17}$$

where $[A]$, $[B]$ and $\{w\}$ are matrices and a vector of known values, respectively, and $\{\eta\}$ represents the unknown vector. In order to solve Eq. (18) in the time domain a θ family of approximation methods will be introduced by using linear interpolation at two time steps as given below:

$$\theta \{\dot{\eta}\}^{n+1} + (1-\theta)\{\dot{\eta}\}^{n} = \frac{\{\eta\}^{n+1} - \{\eta\}^{n}}{\Delta t} 0 \leq \theta \leq 1. \tag{18}$$

By putting different values for θ, various time-marching schemes are achieved. The following equation summarizes four different time-marching schemes used in numerical calculations.

$$\theta = \begin{cases} 0 & \text{Forward scheme} \\ 1/2 & \text{Crank} - \text{Nicolson scheme} \\ 2/3 & \text{Galerkin Method} \\ 1 & \text{Backward scheme} \end{cases} \tag{19}$$

where forward and backward difference schemes are conditionally stable, and the other two schemes are unconditionally stable. The following equation gives the discretized form of Eq. (18) obtained using Eq. (19):

$$[\bar{A}]\{\eta\}^{n+1} = [\bar{B}]\{\eta\}^{n} + \{W\}^{n+1}, \tag{20}$$

where

$$[\bar{A}] = [A] + \theta \Delta t [B],$$
$$[\bar{B}] = [A] - (1-\theta)\Delta t [B]. \tag{21}$$

The desired time marching scheme is initiated from a starting time, and is repeated up to a desirable final time. In this regard, more information is provided in [19]. In this paper, all presented time marching schemes are examined via the 2-D aeroelastic model based on VLM, whereas the 3-D aeroelastic model based on BEM is solved using backward scheme only.

NUMERICAL RESULTS

The numerical results are presented for a typical section airfoil shown in Figure 1, and characterized by the values in Table 1. Also, a relatively high aspect ratio

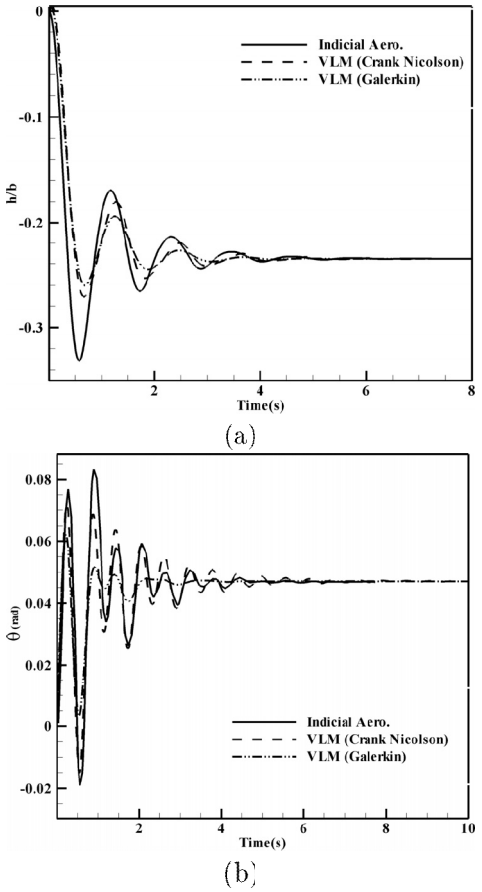

Figure 4. Subcritical dynamic responses of the airfoil subjected to a sharp edge gust ($U_g = 0.738 U_f$) based on different 2-D aerodynamic theories; (a) plunging, (b) pitching.

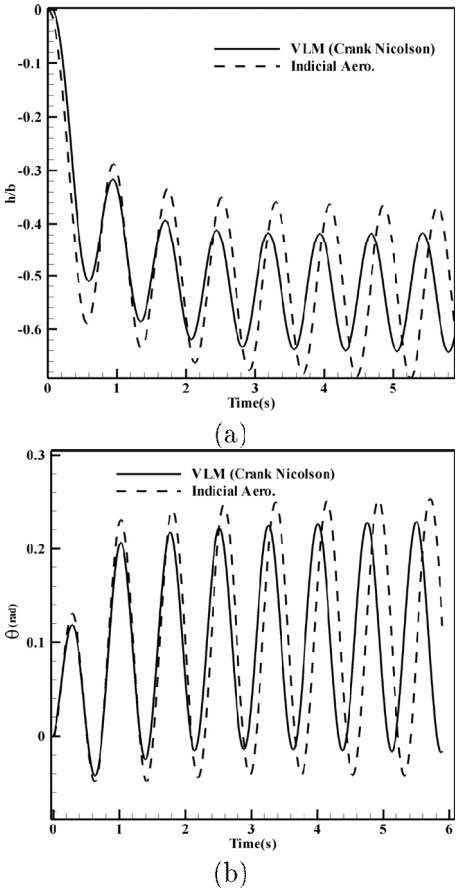

Figure 5. Critical dynamic responses of the airfoil subjected to a sharp edge gust ($U_g = 0.738 U_f$) based on different 2-D aerodynamic theories; (a) plunging, (b) pitching.

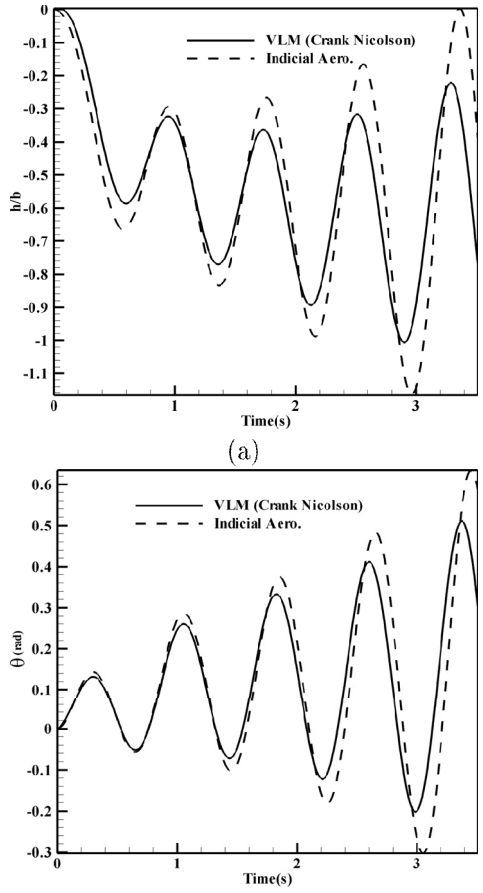

Figure 6. Supercritical dynamic responses of the airfoil subjected to a sharp edge gust based ($U_g = 0.738\,U_f$) on different 2-D aerodynamic theories; (a) plunging, (b) pitching.

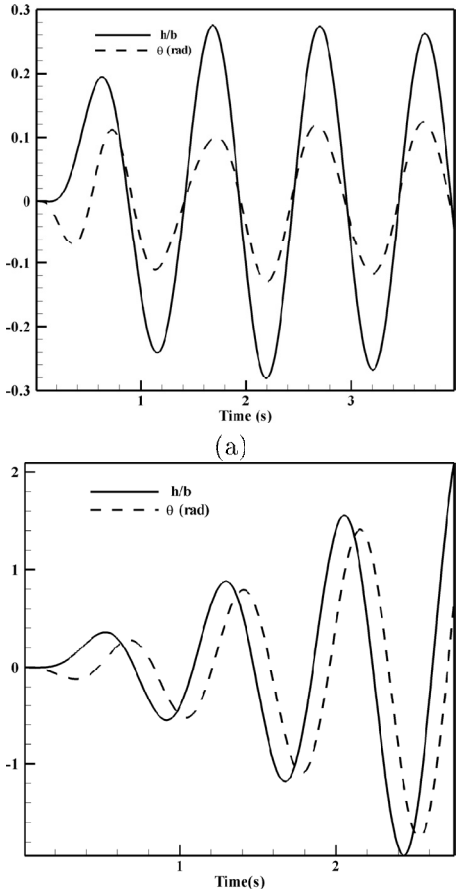

Figure 7. Pitching and plunging responses of the airfoil subjected to a sin profile gust; (a) subcritical, (b) supercritical.

wing with the same non-dimensional cross sectional characteristics as the airfoil is used within the 3-D aeroelastic model based on the BEM to show the accuracy and reliability of the 2-D aeroelastic models in flutter and gust response determination. Here, the subcritical, critical and supercritical conditions correspond to the conditions where the flow velocity is lower, equal and higher than the flutter speed, respectively.

Table 1. Non-dimensional characteristics of the airfoil.

Parameter	Description	Value
$\sigma - \frac{\omega_h}{\omega_\theta}$	The bending-torsion frequency ratio	0.4
a	The elastic axis location	-0.2
$x_\alpha = \frac{S_\alpha}{mb}$	The dimensionless static unbalance	0.1
$\mu - \frac{m}{\pi\rho b^2}$	The density ratio	20
$r_\alpha^2 = \frac{I_\alpha}{mb^2}$	The dimensionless radius of gyration	0.25

Table 2. Non-dimensional flutter speed obtained with different methods.

	Indicial Aero.	VLM	Peters *et.al.* [16]	BEM
$\frac{U_f}{b\omega_\theta}$	2.168	2.182	2.165	2.48
$\frac{\omega_f}{\omega_\theta}$	0.644	0.675	0.655	0.636

In the first part of results, the non-dimensional flutter speed and non-dimensional corresponding frequency are given in Table 2. The numerical values of the parameters are given in Table 1. For the 3-D model, a wing with a relatively high aspect ratio ($AR = 7$) is used, and the cross-sectional characteristics are set to be the same as the airfoil. As seen, the results given by the 2-D models as well as the previous work by Peters *et.al.* [16] show a reasonable agreement with each other for both non-dimensional flutter speed and the non-dimensional corresponding frequency. However, it is quite interesting that the 3-D model based on BEM predicted higher (non-dimensional) flutter speed and lower (non-dimensional) frequency. In fact the values given by 2-D and 3-D models are in a reasonable range, and fortunately the 2-D models give lower values, which result in an overestimate of the flutter speed.

Figure 3 shows how different time marching schemes can change the subcritical dynamic response

for the 2-D aeroelastic model based on VLM. It is seen from the figure that the forward scheme gives a really different behavior relative to the other schemes. In fact, the stability of the finite difference schemes as applied to linear partial differential equations can be investigated by performing Von Neumann stability analysis (also known as Fourier stability analysis) [20]. Indeed, all the schemes could predict almost the same response frequency and also, converging behavior for both the plunging and pitching motions.

In the next set of results (Figures 4 to 6), the aeroelastic models based on Indicial Aerodynamics and VLM have been compared through the subcritical ($U = 0.75U_f$), critical ($U = U_f$) and supercritical ($U = 1.05U_f$) responses due to the sharp edge gust. The gust intensity is $U_g = 0.0738U_f$. These figures show that the Crank Nicolson and Galerkin schemes are closely in agreement with the analytical results obtained via indicial aerodynamics in both transient and steady state responses. Also, this set of figures confirms the converging, limit-cycling and diverging forms of responses for subcritical, critical and supercritical conditions, respectively.

The next figure (Figure 7) simply gives the subcritical and supercritical dynamic responses of the airfoil obtained through the model constructed by using VLM when a sin-profile gust impacts it. Here, it is assumed that the sin-profile gust has the same intensity as the sharp edge gust used in the previous numerical results. Oscillations in both plunging and pitching directions are presented in the figure. It is quite clear that the frequencies of responses in the plunging and pitching directions are almost the same as each other whereas this is not true for the results shown in the previous figures. There (for the sharp edge gust responses), the pitching frequency usually is higher than the frequency of oscillations in the plunging direction.

The last group of figures (Figure 8 and 9) includes the subcritical and supercritical responses of the wingtip given by BEM. Generally speaking, the responses frequencies and amplitudes are lower in case of results provided by 3-D model than the results given by the 2-D models (compare Figure 8 with Figure 4 and Figure 5 with Figure 9). Also, it seems that in the subcritical condition (see Figures 4 and 8) the 2-

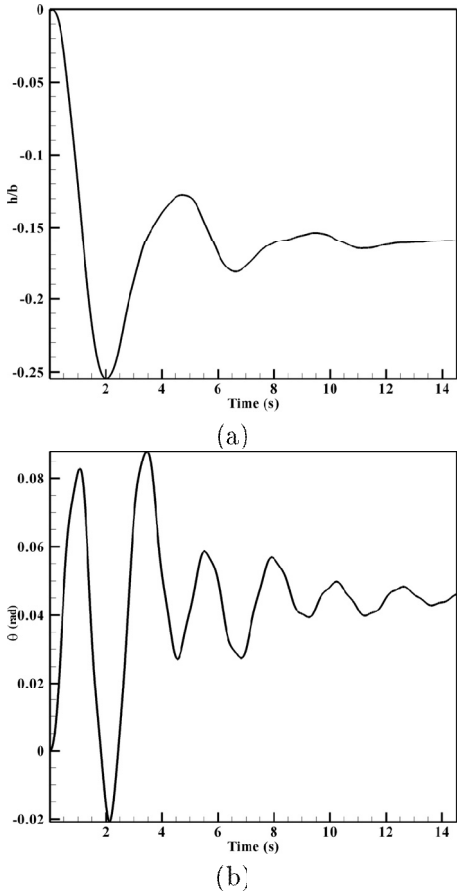

Figure 8. Subcritical dynamic responses of the wingtip subjected to a sharp edge gust ($U_g = 0.738\,U_f$) using BEM; (a) plunging, (b) pitching.

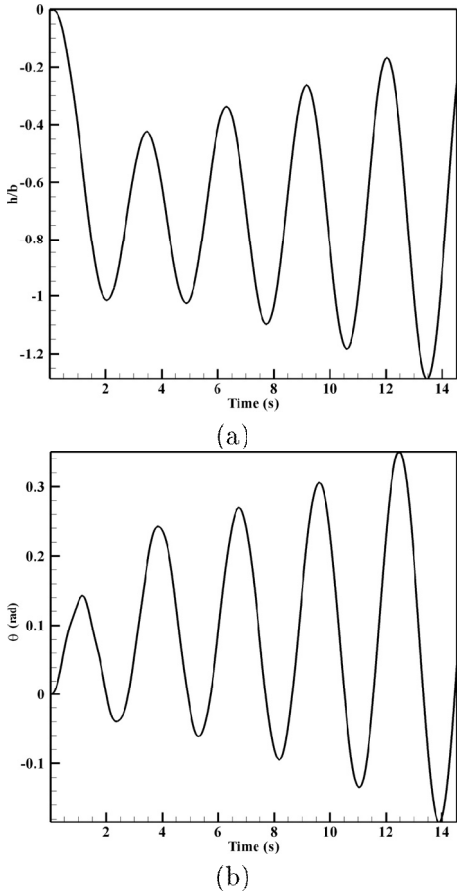

Figure 9. Supercritical dynamic responses of the wingtip subjected to a sharp edge gust ($U_g = 0.738\,U_f$) using BEM; (a) plunging, (b) pitching.

D aeroelastic models take more damping into account than the 3-D model, and that's why they converge more quickly. Moreover, in case of the supercritical condition, one can say that the 2-D models impose higher negative damping values than to the 3-D aeroelastic model.

CONCLUSION

First, two different aerodynamic theories including Indicial Aerodynamics and Vortex lattice Method (VLM), which can be used to make 2-D aeroelastic models, have been reviewed. Then, a 3-D aeroelastic framework made of Boundary Element Method (BEM) and Modal technique has been presented. This model has been used to verify and show the reliability and performance of the 2-D models to find the stability margin and dynamic responses to the gust. Latter, a veriety of numerical results has been generated to present, *e.g.* the effects of different time marching schemes on predicting the dynamic responses of the airfoil entering the sharp edge gust. Also, some comparisons have been made between the 2-D aeroelastic models and the 3-D model. These show that if the 2-D aeroelastic models based on either Indicial Aerodynamics or VLM are used in the preliminary design steps, the design would be on the safe side since they overestimate the instability onset and the dynamic responses.

REFERENCES

1. Theodorsen T., "General Theory of Aerodynamics Instability and Mechanism of Flutter", *NACA Report 496*, (1935).
2. Bisplinghoff R.L., Ashley H., Halfman R.L., *Aeroelasticity*, Dover Publications, (1996).
3. Katz J., Plotkin A., *Low speed aerodynamics*, McGraw-Hill, (1991).
4. Hess J.L., "Review of integral equation techniques for solving potential flow problems with emphasis on the surface source method", *Computer Methods in Applied Mechanics Engineering*, **5**, PP 145-196(1975).
5. Morino L., Chen. L.T. and Suciu E.O., "Steady and Oscillatory Subsonic and Supersonic Aerodynamics around Complex Configurations", *AIAA Journal*, **13**(3), PP 368-374(1975).
6. Behbahani-Nejad M., "Reduced order modeling of 3D unsteady flows using fluid eigenmodes and boundary element method", Ph.D. Dissertation, University of Tehran, Tehran, Iran, (2002).
7. Behbahani-Nejad M., Haddadpour H. and Esfahanian V., "Reduced Order Modeling of Unsteady Flows without Static Correction Requirement", *Journal of Aircraft*, **42**(4), PP 882-886(2005).
8. Shahverdi H., Nobari A. S., Behbahani-Nejad M. and Haddadpour H., "An efficient reduced-order modeling approach based on fluid eigenmodes and boundary element method", *Journal of Fluids and Structures*, **23**, PP 143-153(2007).
9. Davis G.A., Bendiksen O.O., "Unsteady Transonic Two Dimensional Euler Solutions Using Finite Elements", *AIAA Journal*, **31**(6), PP 1051-1059(1993).
10. Batina J.T., "Unsteady Euler Algorithm with Unstructured Dynamic Mesh for Complex Aircraft Aerodynamic Analysis", *AIAA Journal*, **29**(3), PP 327-333(1991).
11. Robinson B.A., Batina J.T., and Yang T.Y., "Aeroelastic Analysis of Wings Using the Euler Equation with a Deforming Mesh", *Journal of aircraft*, **28**(11), PP 781-788(1991).
12. Rausch R.D., Batina J.T., and Yang T.Y., "Three-Dimensional Time-Marching Aeroelastic Analysis Using an Unstructured-Grid Euler Method", *AIAA Journal*, **31**(9), PP 1626-1633(1993).
13. Hall K.C., "Eigen analysis of Unsteady Flows About Airfoils, Cascades, and Wings", *AIAA Journal*, **32**(12), PP 2426-2432(1994).
14. Romanowski M.C., and Dowell E.H., "Using Eigen modes to form an efficient Euler based Unsteady Aerodynamics Analysis", *ASME International Mechanical Engineering Congress and Exposition*, Chicago, (1994).
15. Esfahanian V., Behbahani-Nejad M., "Reduced Order Modeling of Unsteady Flows About Complex Configurations Using the Boundary Element Method", *Journal of Fluids Engineering*, **124**(4), PP 988-993(2002).
16. Hodges D.H., Pierce G.A., *Introduction to Structural Dynamics and Aeroelasticity*, Cambridge University Press, (2002).
17. Sears W.R., and Sparks B.O., "On the Reaction of an Elastic Wing to Vertical Gusts", *Journal of the Aeronautical Sciences*, **9**(2), PP 64-51(1941).
18. Anderson J.D., *Fundamentals of Aerodynamics*, 2nd edition, McGraw-Hill Inc., (1991).
19. Reddy J.N., *An introduction to the finite-element method*, 2nd edition, McGraw-Hill Inc., (1993).
20. Smith G.D., *Numerical Solution of Partial Differential Equations: Finite Difference Methods*, 3nd edition, Oxford University Press, (1985).